Theory and Experimental Evidence of Electroconvection around Electrochemical Deposits

V. Fleury, J.-N. Chazalviel, and M. Rosso
Laboratoire de Physique de la Matière Condensée, Ecole Polytechnique, 91128 Palaiseau, France
(Received 7 October 1991)

We propose a model for the motion of the fluid flow, for the electric field, and for the concentration map around the branches during electrodeposition of ramified metal clusters in two-dimensional cells. This model accounts for the observed distribution of ions in the solution around the metal tips.

PACS numbers: 68.70.+w, 47.15.Hg, 81.15.Lm, 82.45.+z

Electrochemical deposition consists of growing a metallic cluster in an electrochemical cell filled with a solution of a salt of the metal, by imposing a constant current, or potential difference, between the electrodes. We restrict ourselves to thin rectangular cells and constant current. The theory can be extended to other cases. At the cathode, the reaction is

$$M^{z+} + ze^- \rightarrow M_{\text{deposit}} \quad (1)$$

(M is the metallic ion, z^+ its charge, and e^- the electron). The morphology of the deposit depends on the current density J. A forestlike deposit grows on the cathode for $J > J_0 \approx 1$ mA/cm^2. The "trees" look tortuous and "fractal" for $J < 20$ mA/cm^2, and look parallel and vertical for $J > 40$ mA/cm^2. Considerable effort [1–19] has been devoted to understanding the growth regimes of the deposits as a function of relevant parameters. The early work in the field [2–5] was triggered by a possible relationship between the deposits observed at low J and the diffusion-limited aggregates [20,21]. Recently a model [12–14] and experiments [13–18] focusing on the high-J regime have addressed the problem of the interplay of the electric and the diffusion fields of the two kinds of ions. This model [12] is an exact solution of the motion of the ions around an array of branches which are growing in a steady solution (hydrodynamical effects are ignored). It predicts two fundamental facts: (i) The growth speed of the deposit is the speed at which the anions withdraw from the deposit. That is, $\mathbf{v}_a = -\mu_a \mathbf{E}_{\text{bulk}}$, where μ_a is the mobility of the anion and $\mathbf{E}_{\text{bulk}}$ the field in the electrolyte facing the branches. (ii) There exist positive charges at the tips of the branches (over a distance of about 1 μm). However, the concentration gradients as described by this model do not correspond to the observed ones [15–17]. We show in this Letter that the charges at the tips can provoke convective motion of the fluid, and that the solution of the coupled electrical and hydrodynamical problems, when neglecting diffusion, leads to a concentration map which is of the experimentally observed shape. In the following, we first calculate the streamlines of the fluid. We then derive the electric field and the concentration map around the deposit. This will lead to a concentration map with two zones: a zone free of ions and a zone of constant concentration. The sharp gradient at the virtual interface between the two zones is expected to be widened by diffusion. We then briefly present some new experimental evidence of the existence of fluid motion around the tips, and an observation of the concentration gradients during growth which is in agreement with the model, except that the virtual interface is found to be wide.

In order to compute the fluid flow around the deposit, we model the deposit as a comb of rectilinear equally spaced and infinitely thin needles which grow between two plates in a thin layer of electrolyte (see Fig. 1). The comb is infinite and the spacing between the teeth is b. We suppose that the cathode is far behind the deposit, which has already been growing for a while, so that a stationary growth state is reached [12]. It is not necessary to set boundaries in the y direction. Since the deposit is not compact at scales between 0.1 mm and 1 μm, the solution can flow through it. We then make the approximation that the solution flows freely through the needles. The last approximation is to suppose that the charge Q which is found at each tip is pointlike. A local field $\mathbf{E}^*$ is also present there, which is much larger than $\mathbf{E}_{\text{bulk}}$, as expected from the case without convection [12]. Since the charged zone may extend over 1 μm, this approximation seems reasonable: In the 2D approximation we only consider the case where the distance between neighboring trees is larger than the thickness of the cell (200 μm). As a consequence, the fluid experiences a local force $\mathbf{f}$ (in contrast to gravity-driven convection, $\mathbf{f}$ is not a bulk force). $\mathbf{f}$ can be represented as a 2D Dirac vector function located at the tip:

$$\mathbf{f} = Q\mathbf{E}^* \delta(r - r_{\text{tip}}) . \quad (2)$$

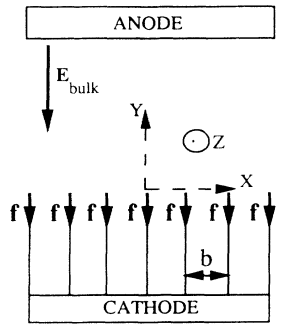

FIG. 1. Schematic view of the cell. The field $\mathbf{E}_{\text{bulk}}$ is constant far ahead. The growth speed is $-\mu_a E_{\text{bulk}}$. A convective motion is driven by the force $\mathbf{f}$ existing at the tips.

It is oriented in the direction antiparallel to growth. We can now solve the Navier-Stokes (NS) equation for this problem (see Fig. 1). As a first step, we determine the fluid flow around a single *motionless* needle, whose tip is located at the origin of the axes. The NS equation in the steady-state regime, and for low Reynolds numbers, is [22]

$$-\nabla P + \nu\Delta \mathbf{v} + \mathbf{f} = 0 \tag{3}$$

($\mathbf{v}$ is the fluid velocity, P the pressure, and ν the dynamic viscosity). Taking the curl of Eq. (3), we write

$$\nu\Delta \mathrm{curl}\mathbf{v} = -\mathrm{curl}\mathbf{f}\,. \tag{4}$$

So far, the speed is a function of the three coordinates x,y,z (see Fig. 1). However, since the cell is very thin, the z dependence of $\mathbf{v}$ can be modeled as a Poiseuille flow [22]:

$$\mathbf{v}(x,y,z) = g(z)\langle \mathbf{v}\rangle(x,y) \text{ with } g(z) = (6/s^2)z(s-z) \tag{5}$$

(s is the thickness of the cell and $\langle \mathbf{v}\rangle$ the average speed along the z direction).

Now, the Laplacian of $\mathbf{v}$ decomposes into two terms:

$$\Delta \mathbf{v}(x,y,z) = g(z)\Delta_2\langle \mathbf{v}\rangle + \langle \mathbf{v}\rangle \frac{\partial^2 g(z)}{\partial z^2}\,, \tag{6}$$

in which Δ_2 is the two-dimensional Laplacian restricted to the x and y variables. In this decomposition, the first term is of order $g(z)v/b^2$ while the second one is of order $g(z)v/s^2$. So, the first term is certainly very small compared to the second one, and can be neglected (this means that variations of $\mathbf{v}$ are expected to be larger in the z direction than in the x-y plane). We now drop the brackets for the average speed in two dimensions. Turning back to the NS equation, we have

$$\nu\,\mathrm{curl}\mathbf{v}(x,y) = -(s^2/12)\mathrm{curl}\mathbf{f}\,. \tag{7}$$

We now introduce the stream vector [22] Ψ, such that $\Psi = (0,0,\Psi(x,y))$, and $\mathbf{v} = \mathrm{curl}\Psi$. Equation (7) leads to

$$\Delta\Psi = \frac{s^2}{12\nu} f \frac{\partial \delta(r)}{\partial x}\,. \tag{8}$$

Noting that Ψ is similar to the vector potential for the magnetic field generated by a distribution along z of magnetic dipoles parallel to y, the solution is

$$\Psi = \frac{1}{2\pi}\frac{s^2}{12\nu} f \frac{x}{r^2}\,. \tag{9}$$

We now calculate the streamlines around a comb. The force is now an array of equally spaced "Dirac forces." The solution is simply analogous to an array of equally spaced lines of dipoles:

$$\Psi = \frac{s^2}{24\pi\nu} f \sum_{k=-\infty}^{k=+\infty} \frac{x-kb}{r_k^2}\,, \tag{10}$$

where r_k is the distance to the tip of rank k.

So far, the comb has been considered to be motionless. We now take into account the fact that the branches grow at a velocity of $\mathbf{v}_a$ by subtracting $\mathbf{v}_a$ from the velocity of the flow. This corresponds to adding a linear term $v_a x$ to the stream function, which becomes

$$\Psi = v_a x + \frac{s^2}{24\pi\nu} f \sum_{k=-\infty}^{k=+\infty} \frac{x-kb}{r_k}\,. \tag{11}$$

This is an almost *exact* solution of the problem of the flow around the growing charged comb, in the limit of low Reynolds number. The streamlines are the constant-Ψ lines; they are shown in Fig. 2. Far away from the tips, forward and backward, the liquid is at rest. In the moving frame, this corresponds to a constant velocity $-\mathbf{v}_a$ parallel to the branches. Between a pair of branches two vortices are formed, which have a singularity at the tips, where the speed of the fluid is infinite. (This singularity could be removed by replacing the ideal line of magnetic dipoles by two current lines parallel to z with a finite spacing; this could also remove the approximation that the branches are infinitely thin.) Another interesting feature of the flow pattern is the largest closed loops of the vortices which separate two zones: one where the fluid is almost translated, and one where it rotates. (One may guess that the ions lying inside the vortices between two branches will be accreted on the tip after drifting in the fluid flow. This could indeed happen in a transient regime; however, we show below that in the steady state the vortices do not contain any ions.)

At first glance, a derivation of both the field and the concentration maps, by solving the full Laplace and drift equations [12] coupled to the NS equation, seems a formidable task. However, since anions do not deposit, and

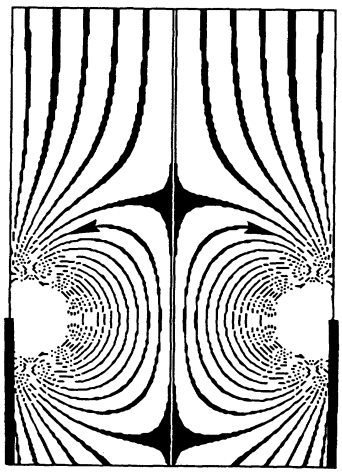

FIG. 2. The pattern for the streamlines, in the moving frame. Two vortices located between two neighboring branches are represented. The pattern is periodic along the x direction. The anions must be frozen in the moving frame, so that the charges at the tips do not increase. The largest loops of the vortices form an arch which is necessarily a field line and the limit below which no ions are found.

since the charge at the tips is constant, the anions must be frozen in the moving frame. This implies that wherever anions are found in the solution, the field is such that $-\mu_a \mathbf{E}+\mathbf{v}=0$. As a consequence, two zones will exist around the deposit: (1) a zone containing anions where $\mu_a \mathbf{E}=-\mathbf{v}$, and (2) a zone free of anions, and hence of cations, where the actual shape of the electric field does not matter.

Diffusion effects can be neglected in the first zone because the concentrations are constant there, as explained below. However, neglecting diffusion at the frontier between these two zones, where a step of concentration is found, is a rather crude approximation. We shall, however, proceed with this approximation, until we compare the predictions to the experiments. When neglecting diffusion, the frontier between the two zones is a virtual interface: This line must itself be both a field line and a streamline. Since the concentration is uniform far ahead of the deposit, this line must be convex. If we now turn to the fluid flow pattern, we see that the only field line ahead of the deposit which is convex is the arch formed by the largest closed loops of the vortices; the zone containing the anions is necessarily on the upper side. As a consequence, in the moving frame, the two zones mentioned above are (1) the zone on the upper side of the arch, which acts as a funnel for the cations, and in which the anions are frozen (Fig. 3); and (2) the vortices themselves, which are empty of ions of both kinds.

The arch itself is composed of two field lines which end up on two tips. Now, the concentration of both cations and anions in the funnel is equal to the bulk concentration C_0. Indeed, the water being incompressible, the flux of fluid is conserved in the funnel, and the flux of $\mathbf{E}$ is also conserved. The conservation of the flux of cations implies that the concentration is equal to C_0. The concentration of anions is identical to the concentration of cations because of electroneutrality.

In the funnel, the field and streamlines are identical. The field lines that would exist between a comb and a flat anode in a neutral medium do not have such a shape. Now, this peculiar shape must be achieved by some specific distribution of charges along the arch, bringing the normal component of the field along the arch to zero. The model then predicts the existence of charges along the virtual interface between the solution containing ions and the vortices. These charges may add a new convective force acting on the fluid; this force is certainly much weaker than the one acting at the tip because the field is much larger at the tip. Inside the vortex the field line pattern is obtained by simply superimposing the solution of the electrical problem without the charges, and the perturbation caused by the charges.

The predictions of this simplified model of growth are as follows: (1) There exist convective vortices between the tips; (2) ahead of the vortices the electric field is proportional to the fluid velocity, in the moving frame; (3) there exists a depleted zone below the arches; (4) the concentration in the funnel is equal to the bulk concentration; and (5) there is a distribution of charges along the arch, which is a virtual interface.

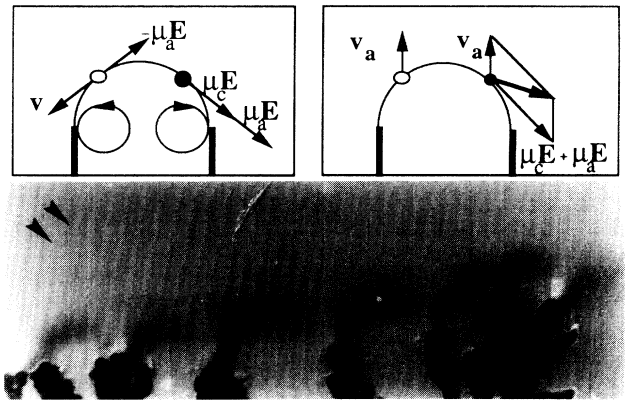

FIG. 3. Experimental observation of the arches during growth of copper sulfate, 5×10^{-2} moll^{-1}. The geometry of the cell is 1.8 mm×1.4 mm×0.1 mm, and the electrodes are along the larger side. A constant potential of 5 V was applied. The interferential contrast allows us to see the concentration gradients. The figure must be viewed as a shadow picture of the concentration profile; the fictitious spotlight direction is indicated by an arrow. The concentration is equal to the bulk concentration on the upper side of the arches, and to zero below the arches. The drawing shows the velocity of an anion and of a cation, in the moving frame (left) and in the laboratory frame (right). Inside each diagram, the anion is sketched on the left, and the cation on the right. The anions are frozen in the moving frame, and are merely translated with a velocity $-\mu_a \mathbf{E}_{\text{bulk}}$ in the laboratory frame. The velocity of the cations is $(\mu_a+\mu_c)\mathbf{E}$ in the moving frame, and $(\mu_a+\mu_c)\mathbf{E}-\mu_a \mathbf{E}_{\text{bulk}}$ in the laboratory frame.

Let us note that, as pointed out by Bruinsma and Alexander [23], the force on the fluid is not expected to initiate convection when the interface is flat, because it is oriented in the wrong direction. However, as soon as the tips exist, the charge is no longer located along a flat interface, and an order-of-magnitude estimate shows that the force is strong enough to initiate convection [24]. Let us note also that decreasing the force at the tips, and hence the speed in the vortex, makes the arches flatter [24].

Previous experimental observations of concentration maps around the tips have appeared in Refs. [15–18]. The arches were seen in the particular case of a dark anion [17,18], namely, (Naphtol-blue-black)$^{--}$, and copper as cation. We report in this Letter new evidence of the existence of the arches in a standard case. We have photographed growths from a solution of copper sulfate (5×10^{-2} moll^{-1}) under a microscope (Nikon104) with Nomarski interferential contrast which allows us to see refractive index gradients. Since the refractive index of the solution increases with increasing concentration,

this allows us to actually see the concentration gradients. An example of the resulting pictures is shown in Fig. 3: The arches clearly appear, and their shape depends on the speed of the vortex below. This speed is not uniquely determined, which seems sensible since the charges at the tips and the local field depend on how advanced a tip is. The vortices were also seen, though their pattern could not be quantitatively compared to the predicted ones. Let us note that the tip of the branches is a very active zone because of the high speed of the fluid which goes through the deposit. Of course, the observed speed is not infinite. As expected the observed arch is not infinitely steep, since diffusion will spread over a finite length the sharp virtual interface which would otherwise exist. However, the simple model presented here captures the main features of the steady state. In principle, the theory presented here can be extended to any distribution of tips and forces (possibly fractal) by changing the driving term in Eq. (8).

Let us stress the following point: Each time a branch undergoes tip splitting, a pair of vortices are created. Each time a branch dies, a pair of vortices disappear. It is possible that the average spacing between trees, and hence the morphology of the deposit, is determined by the characteristic size of the vortices. The latter is linked to the value of the charge at the tip, itself linked to the δV parameter of Refs. [12] and [13]. Work along these lines is in progress. A possible role of Marangoni convection has been conjectured recently [7(b)]. Whatever the origin of the convection, the overall discussion concerning the existence of two zones of different concentrations and the motion of the anions will remain, as soon as a flow pattern is given. However, the concentration profile that we report is at variance with the ones previously reported [15], which may be due to different chemical conditions. Especially, the case of zinc is certainly different because of crystalline anisotropy.

This work was supported by the Centre National d'Etudes Spatiales under Contract No. 89/1229.

[1] R. M. Brady and R. C. Ball, Nature (London) **309**, 225 (1984).

[2] M. Matsushita, M. Sano, Y. Hayakawa, H. Honjo, and Y. Sawada, Phys. Rev. Lett. **53**, 286 (1984).

[3] D. G. Grier, E. Ben-Jacob, R. Clarke, and L. M. Sander, Phys. Rev. Lett. **56**, 1264 (1986).

[4] Y. Sawada, A. Dougherty, and J. P. Gollub, Phys. Rev. Lett. **56**, 1260 (1986).

[5] F. Argoul, A. Arneodo, G. Grasseau, and H. L. Swinney, Phys. Rev. Lett. **61**, 2558 (1988).

[6] D. B. Hibbert and J. R. Melrose, Phys. Rev. A **38**, 1036 (1988).

[7] (a) P. Garik, D. Barkey, E. Ben-Jacob, E. Bochner, N. Broxholm, B. Miller, B. Orr, and R. Zamir, Phys. Rev. Lett. **62**, 2703 (1989); (b) P. Garik, J. Hetrick, B. Orr, D. Barkey, and E. Ben-Jacob, Phys. Rev. Lett. **66**, 1606 (1991).

[8] J. R. Melrose and D. B. Hibbert, Proc. R. Soc. London A **423**, 149–158 (1989).

[9] G. L. M. K. S. Kahanda and M. Tomkiewicz, J. Electrochem. Soc. 136, 1497 (1989).

[10] M. Matsushita, in *Experimental Observation of Aggregations, the Fractal Approach to Heterogeneous Chemistry*, edited by D. Avnir (Wiley, New York, 1989).

[11] Yasuji Sawada and Haruhiko Hyosu, in *Proceedings of the International Conference Honouring Benoit B. Mandelbrot on his 65th Birthday* [Physica (Amsterdam) **38D**, 299–303 (1989)].

[12] J.-N. Chazalviel, Phys. Rev. A **42**, 7355–7366 (1990).

[13] V. Fleury, J.-N. Chazalviel, M. Rosso, and B. Sapoval, J. Electroanal. Chem. **290**, 249 (1990).

[14] J. R. Melrose, D. B. Hibbert, and R. C. Ball, Phys. Rev. Lett. **65**, 3009 (1990).

[15] D. P. Barkey, J. Electrochem. Soc. **138**, 2912 (1991); D. P. Barkey and P. D. Laporte, J. Electrochem. Soc. **137**, 1655 (1990).

[16] M. Rosso, V. Fleury, J.-N. Chazalviel, B. Sapoval, and E. Chassaing, in *Scaling in Disordered Materials*, edited by J. P. Stokes, M. O. Robbins, and T. A. Witten, MRS Symposia Proceedings No. EA-25 (Materials Research Society, Pittsburgh, 1990), pp. 245–249.

[17] V. Fleury, J.-N. Chazalviel, M. Rosso, and B. Sapoval, Ann. Chim. Fr. **16**, 143–148 (1991).

[18] V. Fleury, M. Rosso, and J.-N. Chazalviel, Phys. Rev. A **44**, 6693–6705 (1991).

[19] L. Lam, R. D. Pochy, and V. M. Castillo, in *Non-Linear Structures in Physical Systems*, edited by L. Lam and H. C. Morris (Springer, New York, 1990).

[20] T. A. Witten and L. M. Sander, Phys. Rev. Lett. **47**, 1400 (1981).

[21] T. A. Witten and L. M. Sander, Phys. Rev. B **27**, 5686 (1983).

[22] L. Landau and E. M. Lifshitz, *Fluid Mechanics* (Mir, Moscow, 1984).

[23] R. Bruinsma and S. Alexander, J. Chem. Phys. **92**, 3074 (1990).

[24] V. Fleury, M. Rosso, and J.-N. Chazalviel (to be published).

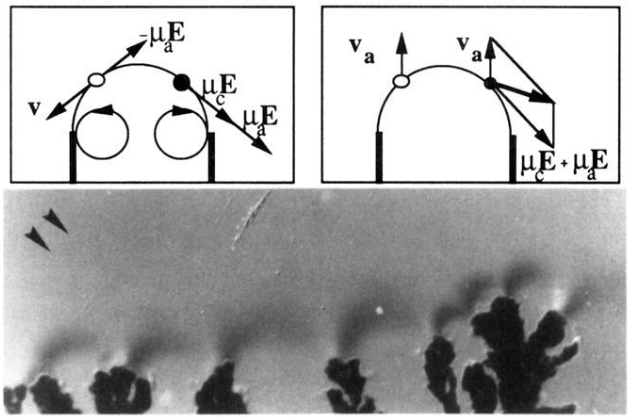

FIG. 3. Experimental observation of the arches during growth of copper sulfate, 5×10^{-2} mol l^{-1}. The geometry of the cell is 1.8 mm × 1.4 mm × 0.1 mm, and the electrodes are along the larger side. A constant potential of 5 V was applied. The interferential contrast allows us to see the concentration gradients. The figure must be viewed as a shadow picture of the concentration profile; the fictitious spotlight direction is indicated by an arrow. The concentration is equal to the bulk concentration on the upper side of the arches, and to zero below the arches. The drawing shows the velocity of an anion and of a cation, in the moving frame (left) and in the laboratory frame (right). Inside each diagram, the anion is sketched on the left, and the cation on the right. The anions are frozen in the moving frame, and are merely translated with a velocity $-\mu_a \mathbf{E}_{\text{bulk}}$ in the laboratory frame. The velocity of the cations is $(\mu_a + \mu_c)\mathbf{E}$ in the moving frame, and $(\mu_a + \mu_c)\mathbf{E} - \mu_a \mathbf{E}_{\text{bulk}}$ in the laboratory frame.